Boundary conditions for incoherent quantum transport

Martin Frey, Aniello Esposito and Andreas Schenk
Integrated System Laboratory
Swiss Federal Institute of Technology Zurich (ETHZ)
CH-8092 Zurich
Email: mfrey@iis.ee.ethz.ch

***Abstract*—In this paper, the influence of coherent and incoherent boundary conditions for quantum transport through silicon nanowires is studied. An iteration scheme to compute an approximate self-energy in the contacts is proposed. The focus lies on the impact on the self-consistent electrostatics and the current computation. In addition, the scaling behavior with increasing device lengths is shown.**

I. Introduction

The Non-equilibrium Green's Function (NEGF) formalism provides a framework to simulate quantum transport in nanoscale devices. It allows the introduction of various scattering mechanisms, such as carrier-phonon scattering or carrier-carrier scattering by a perturbative approach.
With shrinking device length, the effect of the contacts on the device becomes increasingly important. When the device length is of the same magnitude as the coherence length of the carriers, contacts should be considered as reservoirs of *incoherent* carriers. In this paper, we study the effect of coherent and incoherent carrier injection on quantum transport in silicon nanowires including carrier-phonon scattering.

II. Quantum transport equations

Assuming a parabolic band structure for silicon, we express the effective mass Hamiltonian $H(r)$ in the so-called coupled mode expansion [1][2]. The steady-state Dyson equation for the nanowire device then reads as

$$\sum_{n'}\left(E\delta_{n,n'}-\int dr\phi_n^*(r)H(r)\phi_{n'}(r)- \int dr\int dr'\phi_n^*(r)\Sigma^R(r,r')\phi_{n'}(r')\right)G^R_{n',m} = \sum_{n'}(E\delta_{n,n'}-H_{n,n'}-\Sigma^R_{n,n'})G^R_{n',m}=\delta_{n,m}. \quad (1)$$

Carrier-carrier interaction is included in the Hamiltonian via the Hartree potential. The retarded self-energy $\Sigma^R(r,r')$ contains the electron-phonon interaction in the device as well as the boundary conditions:

$$\Sigma^R(r,r')=\Sigma^R_{int}(r,r')+\Sigma^R_{bc}(r,r'). \quad (2)$$

The electron-phonon interaction is approximated as being local in space [3]:

$$\Sigma^<_{i,j}(r,r',E)=\sum_{k,l}C^{\pm}_{i,j,k,l}G^<_{k,l}(r,r',E\pm\hbar\omega)\delta(r-r') \quad (3)$$

$$\Sigma^R_{i,j}(r,r',E)=\frac{1}{2}(\Sigma^>_{i,j}(r,r',E)-\Sigma^<_{i,j}(r,r',E))+ iP\int\frac{dE'}{2\pi}\frac{\Sigma^>_{i,j}(r,r',E')-\Sigma^<_{i,j}(r,r',E')}{E-E'},$$

where $P\int dE'$ is the principal part of the integration which is not neglected in our calculation. The scattering parameters are the same as in [3][4].
The Green's functions, self-energies and electrostatic potential are iterated until self-consistency is achieved.

III. Boundary Conditions

The boundary self-energy in Σ^R_{bc} is directly computed in mode space by calculating the Green's function g^R of an semi-infinite lead, assuming a constant potential:

$$\Sigma^R_{bc}(r_0,r_0,E)=Tg^R(r_0,r_0,E)T, \quad (4)$$

$$g^R(r_i,r_j,E)=MP_iM^{-1}g^R(r_i,r_i,E)MP_j^{-1}M^{-1} \quad (5)$$

where $T=H_{0-1}=H_{-10}$ are the off-diagonal elements of the discretized Hamiltonian which couples site r_0 to r_{-1}, P_i is the discrete propagation factor, and M describes the mode coupling [5][6]. For coherent injection from the lead into the device, $g^R(r_0,r_0,E)$ can be directly computed (i.e. without iterations) using the translational invariance of the Hamiltonian in the lead.
However, in order to model incoherent injection of carriers, a Dyson equation needs to be solved in the lead with an iteration scheme as described in the previous section for the device (except that the Poisson equation doesn't need to be solved for the lead, since the electrostatic potential is assumed constant). The main difference between the iteration scheme used for the leads and for the device is that the Green's functions in the lead are approximated by analytical expressions. This is necessary because the set of equations needs to be closed. In the following, two analytical expressions for the retarded Green's function are given, which are needed in the proposed iteration scheme.
As discussed in [6], the expression for the retarded Green's

978-1-4244-3927-0/09/$25.00 ©2009 IEEE

function of an infinite system $\widetilde{G}^R$ with constant potential $V(r) = V_0$, and the one of a semi-infinite system $\widetilde{g}^R$ with the potential $V(r) = \infty, \forall r \geq L$ and $V(r) = V_0, \forall r < L$, are given by:

$$\widetilde{G}^R_{n,n}(r_i, r_j, E) = -i\frac{m}{\hbar^2 k_n} e^{-ik_n|r_i - r_j|}, \tag{6}$$

$$\widetilde{g}^R_{n,n}(r_i, r_j, E) = -\frac{2m}{\hbar^2 k_n} sin(k_n|r_i - L|) e^{-ik_n|r_j - L|}, \tag{7}$$

where the wave vector k_n is defined as

$$k_n = \frac{\sqrt{2m(E - E_n - \Sigma^R_{n,n})}}{\hbar}. \tag{8}$$

The definition of the wave vector in Eq. (8) is natural in the case of an infinite system because the following relations hold:

$$\widetilde{G}^R(r_i, r_j, E) = \widetilde{G}^R(r_i - r_j, E), \tag{9}$$

$$\Sigma^R(r_i, r_j, E) = \Sigma^R(r_i - r_j, E), \tag{10}$$

and therefore

$$\widetilde{G}^R(r_i, r_i, E) = \widetilde{G}^R(r_j, r_j, E), \tag{11}$$

$$\Sigma^R(r_i, r_i, E) = \Sigma^R(r_j, r_j, E). \tag{12}$$

In the case of the semi-infinite system, the self-energies are position dependent. However, the wave vector k_n in Eq. (8) is only globally defined if this dependency is ignored. By doing so, both the infinite and semi-infinite retarded Green's function can be computed by the knowledge of the retarded self-energy at a single position.

The underlying thought of our iteration scheme for the contacts is the following:

When dividing an infinite system into a finite device and semi-infinite leads, the boundary self-energies Σ^R_{bc} for the device, given in Eq. (4), depend on Green's functions describing the leads when they are not coupled to the device. However, the scattering (or interaction) self-energies Σ^R_{int} in the leads depend on the Green's function of the entire infinite system, i.e. when the leads are coupled to the device. Equations (6) and (7) are used to compute an approximation of the retarded Green's function in the lead (when it is coupled the device) in the presence of scattering. Since thermal equilibrium is assumed within the leads, $\widetilde{G}^<$ and $\widetilde{g}^<$ can be computed from $\widetilde{G}^R$ and $\widetilde{g}^R$ using the fluctuation-dissipation theorem. These approximate Green's functions are used in Eq. (3) to compute the retarded self-energy, which is subsequently used in Eq. (6) and (7) again.

As illustrated in Fig. 1, $\widetilde{G}^R_{n,n}(r_i, r_j, E)$ is used in order to approximate the retarded Green's function, when the energy E is greater than the corresponding subband energy E_n throughout the device:

$$E > E_n(r), \forall r \rightarrow \widetilde{G}^R_{n,n}(r_i, r_j, E). \tag{13}$$

The approximation $\widetilde{g}^R_{n,n}(r_i, r_j, E)$ is used for energies E greater than the subband energy at the boundary $E_n(r_0)$, but

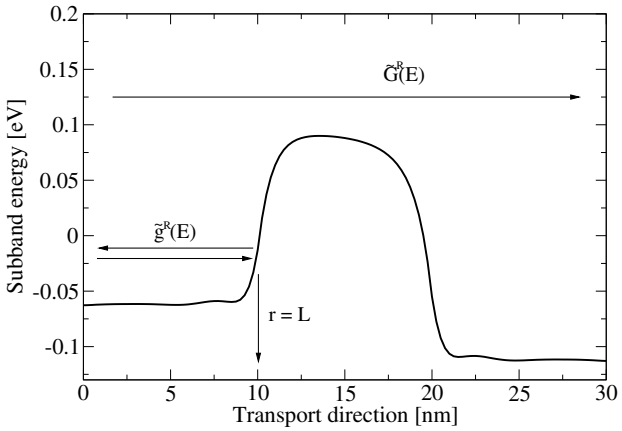

Fig. 1. For energies greater than the maximum of the subband, $\widetilde{G}^R_{n,n}(r_i, r_j, E)$ is used for the contact iteration. In the other case, $\widetilde{g}^R_{n,n}(r_i, r_j, E)$ is used. Coming from the lead, the first point where the energy equals the subband energy is defined as L.

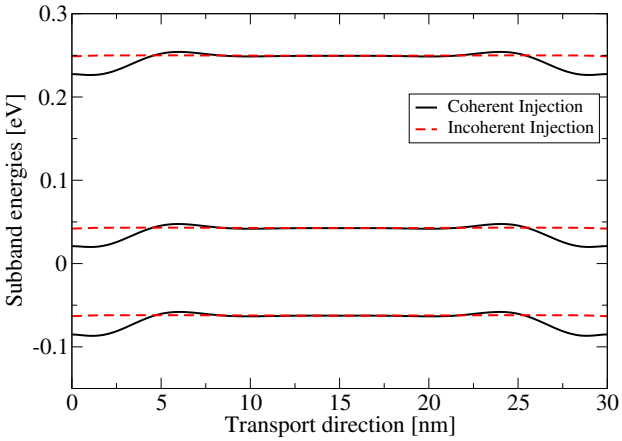

Fig. 2. Subband profile of a *Resistor*, $L_D = 30\,nm$: for coherent injection, a non-physical bending of $25\,meV$ results due to the non-constant DOS.

equal to a subband energy $E_n(L)$ at a certain point L in the device:

$$E_n(r_0) \leq E \leq E_n(L) \rightarrow \widetilde{g}^R_{n,n}(r_i, r_j, E). \tag{14}$$

Naturally, the quality of these approximations depends on the simulated device and will be discussed in the next section.

IV. Results

In order to study the impact of coherent and incoherent carrier injection on the electrostatic solution, two different types of devices are simulated:

1) *Resistor* : A set of Si nanowires with a cross-section of $3 \times 3\,nm^2$ and device lengths between $L_D = 10\,nm$ and $L_D = 50\,nm$ with a homogeneous doping of $2e20\,cm^{-3}$.
2) *MOSFET* : A triple-gate Si nanowire with $L_G = 10\,nm$, total dimension of $3 \times 3 \times 30\,nm^3$, source-drain extensions with a doping of $2e20\,cm^{-3}$ and an undoped channel.

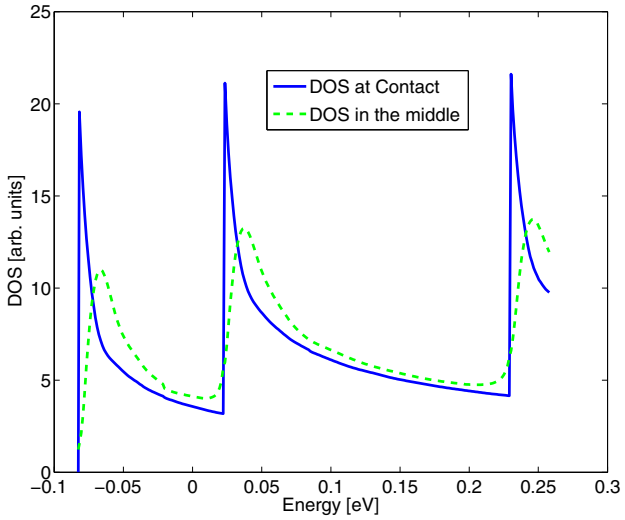

Fig. 3. DOS of the *Resistor*, $L_D = 30\,nm$: Coherent injection, cuts taken at the contact $x = 0$ (blue) and in the middle at $x = 15\,nm$ (green, dashed).

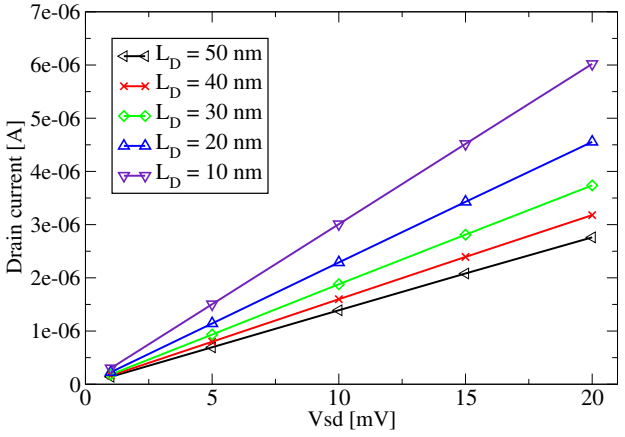

Fig. 4. The current of the *Resistors* as a function of the applied voltage for different device lengths, when simulated with incoherent injection.

In the equilibrium state of a *Resistor* with Ohmic contacts, the electrostatic potential and therefore all subbands must be constant along the transport direction x in the device. This condition is only achieved with incoherent injection while with coherent injection, the density of states (DOS) becomes a function of x. Since the electron-phonon interaction respects the principle of detailed balance, the distribution function is the Fermi function throughout the device. With the distribution function unaltered, a non-constant DOS results in a non-constant density and potential along x.

In Fig. 2 the subband profile for the lowest valley is shown for both injection types. For coherent injection, a non-physical bending of $25\,meV$ results due to the non-constant DOS. With incoherent injection, the subbands are constant, as the DOS is the same everywhere in the device.

In Fig. 3 the DOS at two different sites along the channel is displayed for the case of coherent injection. While the DOS at the device boundary has large peaks because of the coherent contribution, it is smeared out in middle of the device.

For a *Resistor* in equilibrium, our approximation (6) for the retarded Green's function is identical to the exact solution. As soon as a finite bias is applied to a *Resistor*, there is a discrepancy between the exact solution and our expressions in (6) and (7). If the applied bias V_{SD} is small, we expect the current to be a linear function of the voltage. This is shown in Fig. 4 for various device lengths.

In Fig. 5 the scaling behavior of the current of the *Resistors* as a function of their respective device length is shown. All curves in Fig. 5 show a similar behavior, which becomes clearer when plotting the resistance

$$R(L_D) = \frac{V_{SD}}{I_D(L_D)}, \tag{15}$$

defined as the ratio of applied voltage and current, as a function of the device length. This is shown in Fig. 6.

An ohmic resistance is solely defined by the device geometry and its material, and should scale linearly with its length:

$$R \sim L_D. \tag{16}$$

Therefore, if our *Resistors* show ohmic behavior, we would expect that the curves from Fig. 5 collapse to a single straight line, when plotting $R(L_D)$, which is indeed the case for incoherent injection as shown in Fig. 6. Similar plots with coherent injection could not be produced because the unphysical bending of the subbands leads to strong oscillations in the density - potential iteration and a lack of convergence, when a finite bias is applied.

Next the electrostatics of a *MOSFET* with Ohmic contacts in the sub-threshold region at $V_G = 0.1\,V$ and $V_{SD} = 50\,mV$ is investigated. With a barrier several kT above the highest chemical potential, the carriers in the highly doped source/drain extensions should be in equilibrium with their respective contact and the potential must be flat towards the contact, see Fig. 7.

For a fixed *MOSFET* device geometry with small source-drain extensions ($\approx 10\,nm$), the current is almost identical when comparing results from simulations with coherent injections to results with incoherent injection. This is due to the fact that the current of a *MOSFET* is a function of:

1) The height of the barrier, which is controlled by the gate contact.
2) The scattering mechanisms which are present in the device.

As can be seen in Fig. 7, the height of the barrier is essentially the same for coherent and incoherent injection. Naturally, the scattering mechanisms which are present in the device are also the same in both cases. It is therefore not surprising that the drain current of a *MOSFET* is not significantly influenced by the choice of the injection mechanism.

However, if the source-drain extensions become larger ($\approx 20\,nm$), the convergence behavior for coherent injection deteriorates much faster compared to simulations with incoherent injection.

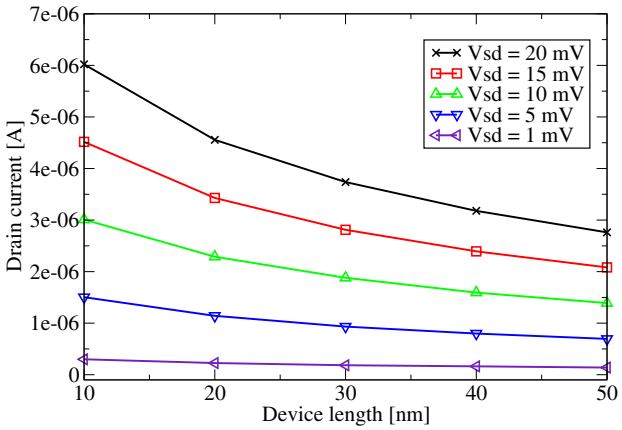

Fig. 5. The current of the *Resistors* as a function of the device length for different applied voltages, when simulated with incoherent injection.

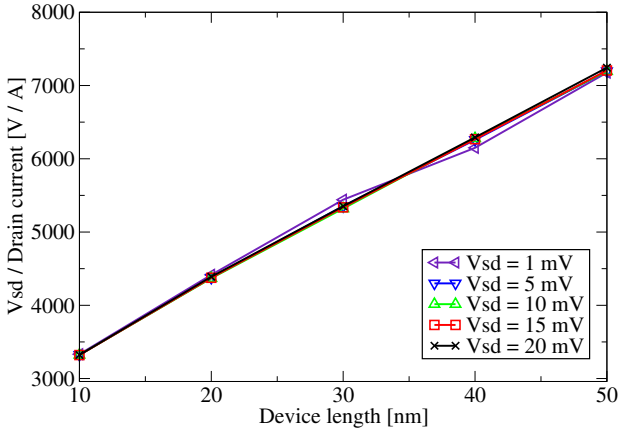

Fig. 6. Plotting the resistance $R(L_D)$ for the curves from Fig. 5, all curves should collapse to a single straight line. All points of one curve are within an interval of 2% around the mean of the points from all other curves. The line with $V_{SD} = 1\,mV$ deviates most from all others, since it is the current of the lowest magnitude and therefore affected most by numerical errors.

V. Conclusion

In quantum transport simulations of devices with carrier-phonon interaction, the injection of coherent carriers leads to an artificial bending of the bands. Physically reasonable band shapes are achieved by the injection of incoherent carriers. This requires an additional iterative loop, as outlined in Section III. With incoherent injection, an ohmic behavior can be observed when scaling the device length.

Acknowledgment

The authors would like to thank S. Steiger and Dr. M. Luisier for interesting discussions and hints. This work had financial support by the EU project IST-216171-NANOSIL.

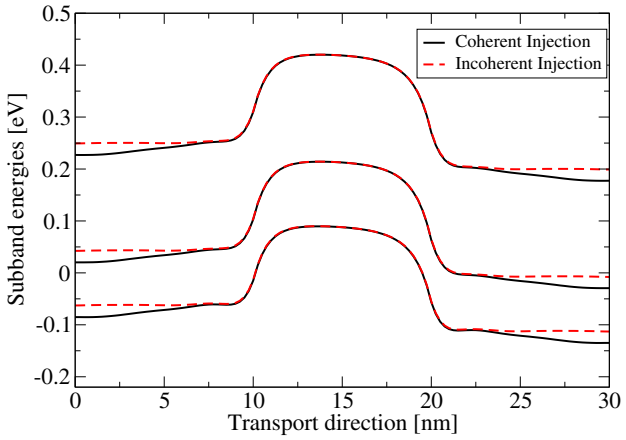

Fig. 7. Subband profile of the *MOSFET* at $V_G = 0.1\,V$ and $V_{SD} = 50\,mV$: As in the case of the *Resistor*, a subband bending of about $25\,meV$ occurs for coherent injection.

References

[1] R. Venugopal, Z. Ren, D. Jovanovic, S. Datta and M. Lundstrom, *J. Appl. Phys.*, vol 92, 3730, 2002

[2] S. Datta, *Electronic transport in mesoscopic systems* (Cambridge University Press, New York, 1995)

[3] S. Jin, Y. Park and H. S. Min, *J. Appl. Phys.*, vol 99, 123719, 2006

[4] C. Jacoboni and L. Reggiani, *Rev. Mod. Phys.*, vol 55, 645, 1983

[5] R. Lake, G. Klimeck, R. C. Bowen and W. R. Frensley, *Phys. Rev. B*, vol 52, 4, 1995

[6] M. J. McLennan, Y. Lee and S. Datta, *Phys. Rev. B*, vol 43, 17, 1991